Supplementary Information

Rechargeable Nickel Telluride/Aluminum Batteries with High Capacity and Enhanced Cycling Performance

Zhijing Yu,[†] Shuqiang Jiao,[,†] Jiguo Tu,[†] Yiwa Luo,[†] Wei-Li Song,*[,‡] Handong Jiao,[‡] Mingyong Wang,[†] Haosen Chen*[,‡] and Daining Fang[‡]*

[†] State Key Laboratory of Advanced Metallurgy, University of Science and Technology Beijing, Beijing 100083, P. R. China.

[‡] Institute of Advanced Structure Technology, Beijing Institute of Technology, Beijing 100081, P. R. China.

*E-mail addresses: sjiao@ustb.edu.cn (S. Jiao); weilis@bit.edu.cn (W. L. Song); chenhs@bit.edu.cn (H. Chen).

Table S1 Comparison of the electrochemical performance of the NiTe electrode with reported works

Positive electrode		Current density ($mA\ g^{-1}$)	Capacity ($mA\ h\ g^{-1}$)	Discharge potential (V)
		200	570	
This work	NiTe	500	445	1.3
		1000	211	
Graphitic Carbon paper[1]		50	89.9	1.8
Defect-Free-GA3000[2]		5000	80	2.25
Graphene Microflowers[3]		5000	100	1.85
Graphene Nanoribbons[4]		5000	123	2.1
V_2O_5[5]		125	305	0.6
VO_2[6]		50	165	0.5
TiO_2[7]		20	100	0.5
S[8]		20	1600	1.3
NiS[9]		200	106.9	1.15
CuS[10]		20	240	1.0
SnS_2[11]		100	400	0.7
Se[12]		600	330	1.52
Cu_2-xSe[13]		100	241	0.5
Cu_3P[14]		50	73.8	0.7
		20	913	
Te[15]		50	591	1.5
		500	400	

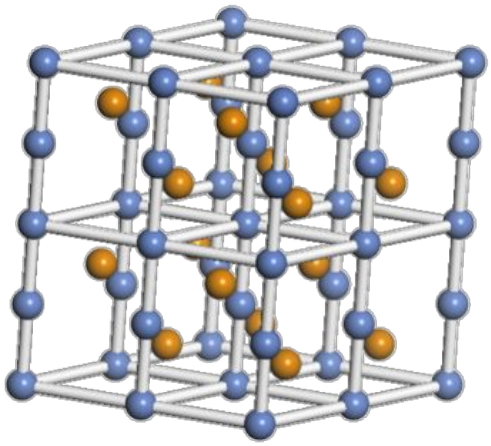

Figure S1 Schematic representation of NiTe crystal structure.

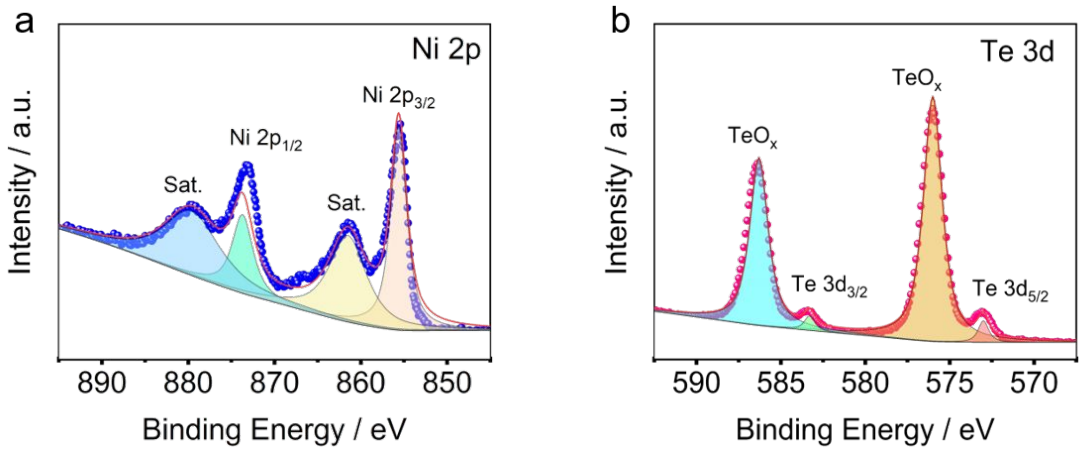

Figure S2 XPS spectra of the as-prepared NiTe. (a) Ni 2p (b) Te 3d.

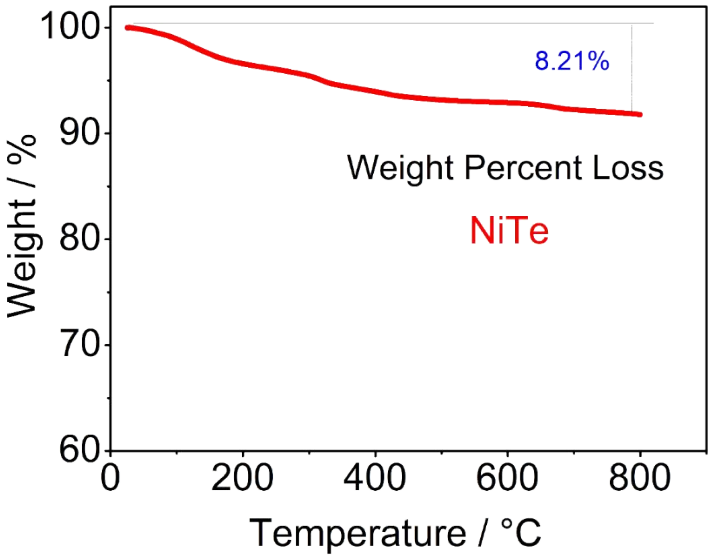

Figure S3 TG curves of the as-prepared NiTe.

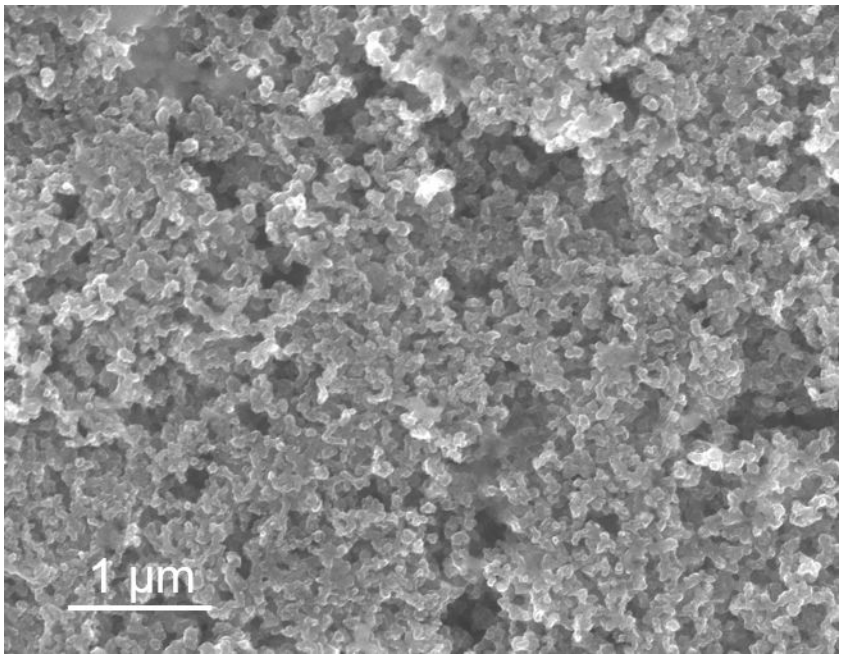

Figure S4 FE-SEM image of the positive electrode plate.

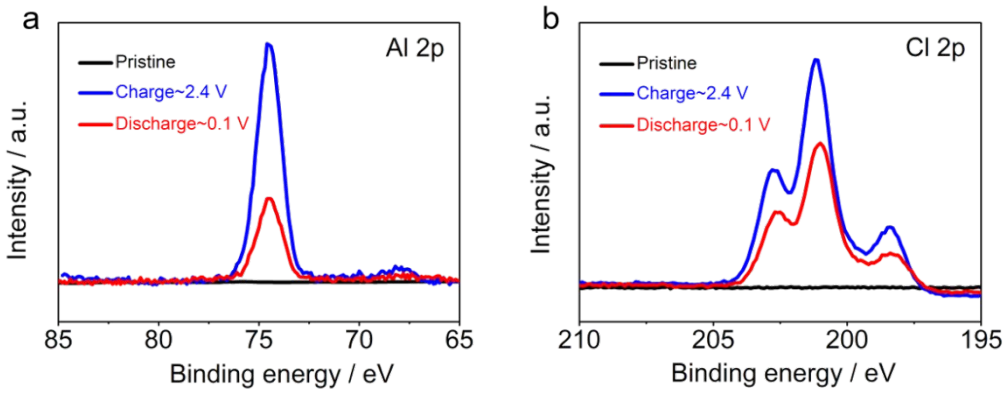

Figure S5 XPS spectra of (a) Al 2p (b) Cl 2p at different states.

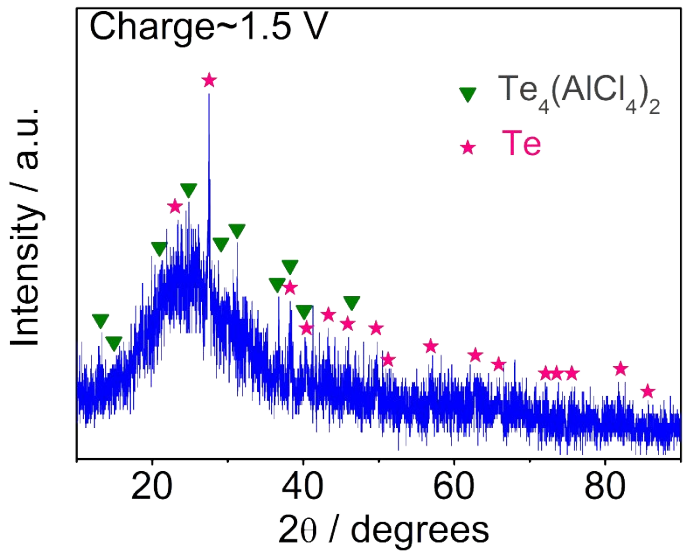

Figure S6 XRD of the NiTe positive electrode charged to 1.5 V.

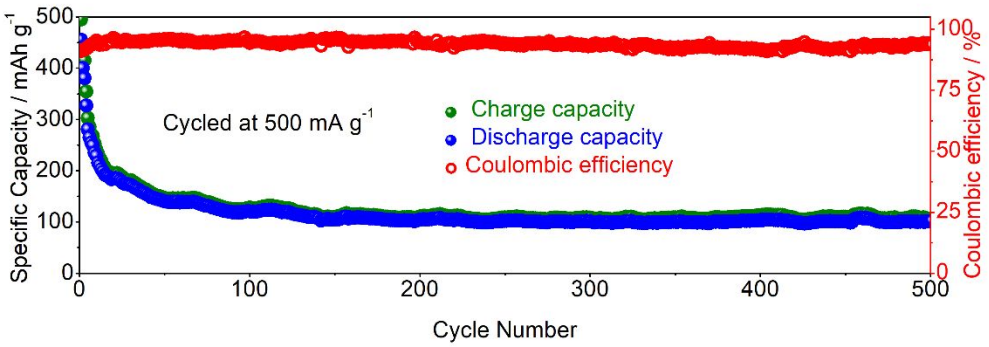

Figure S7 Cycling performance of the Al/NiTe battery at a current density of 500 mA g^{-1}.

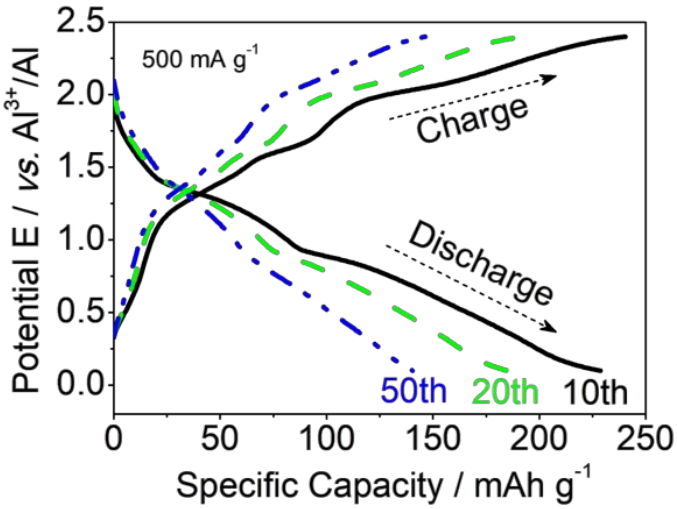

Figure S8 Charge and discharge curves from 10th to 50th cycle at the current density of 500 mA g^{-1}.

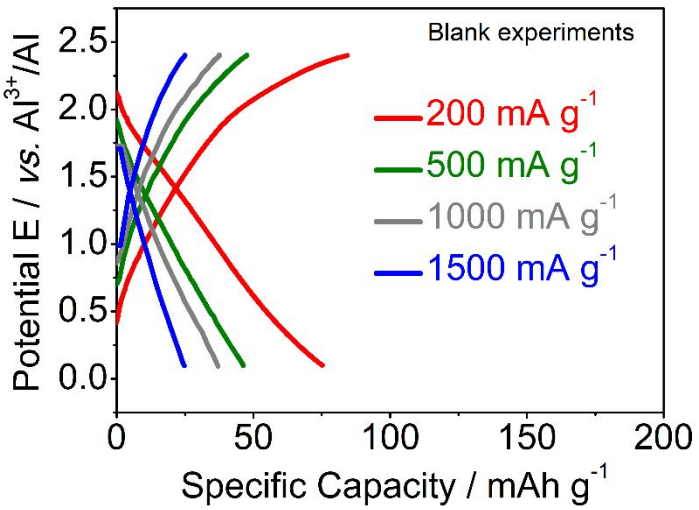

Figure S9 Charge and discharge curves of the blank batteries at different current densities.

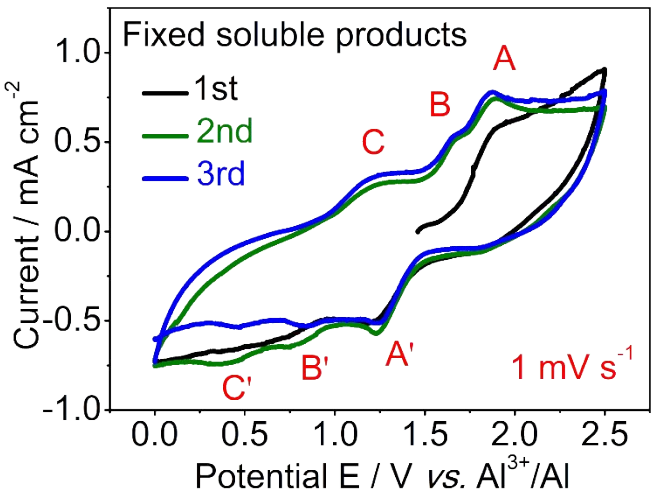

Figure S10 Cyclic voltammograms of the battery with a modified separator at a scan rate of 1 mV s^{-1} between 0~2.50 V *vs* Al/Al^{3+}.

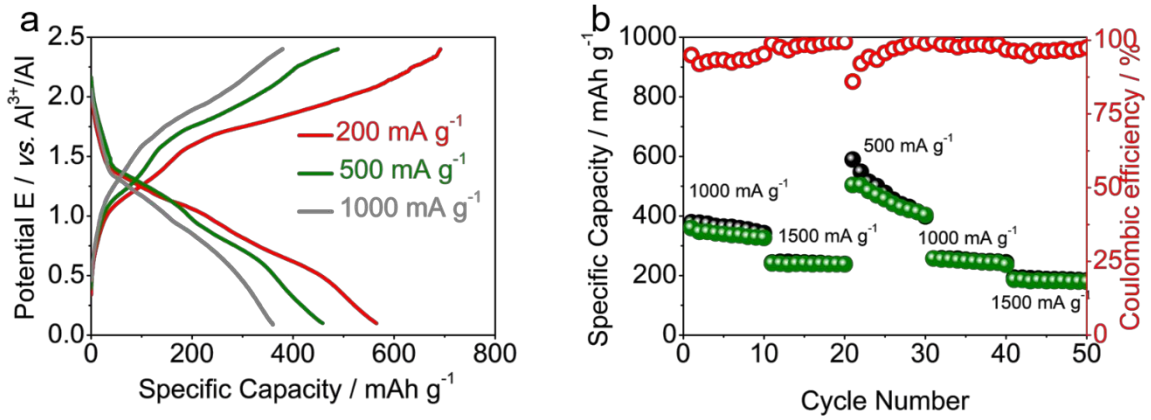

Figure S11 (a) Charge and discharge curves of the modified batteries at different current densities. (b) Rate performance of the modified batteries.

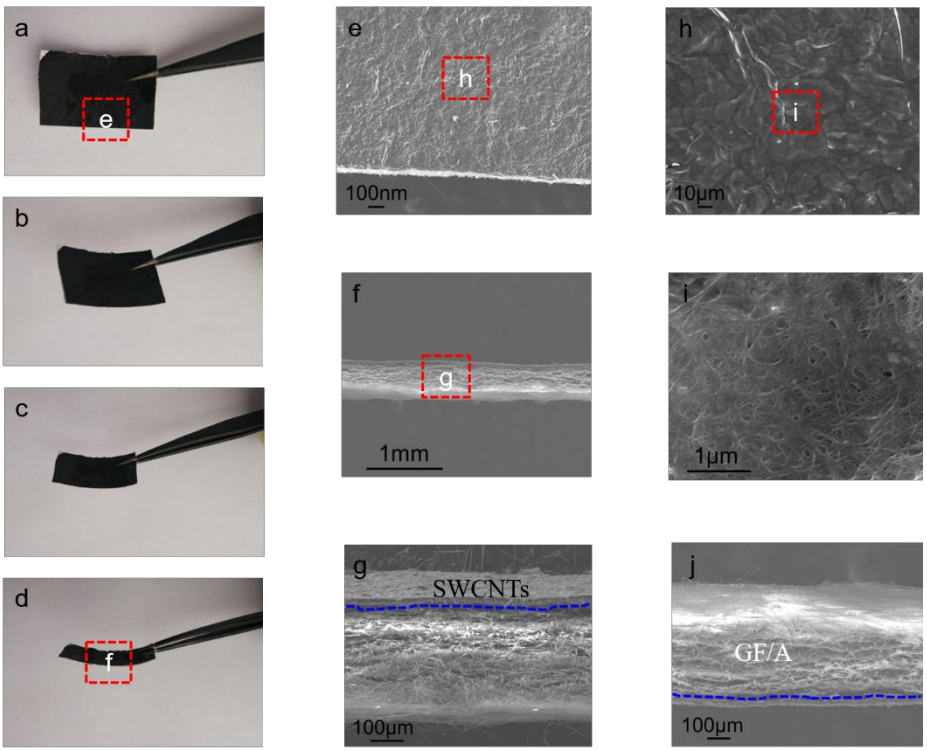

Figure S12 Modified separator after the cycling test (a-d) Photos. (e-j) Corresponding SEM images.

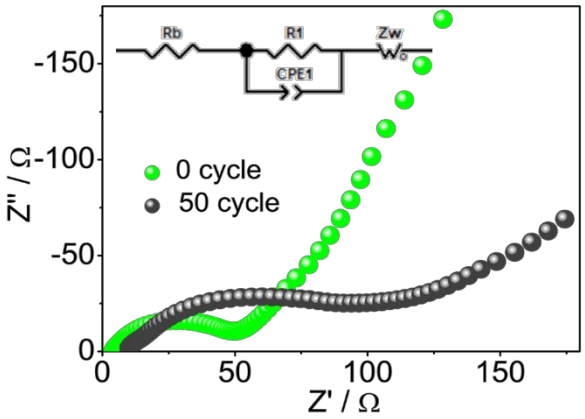

Figure S13 Nyquist plots of Al/NiTe battery before cycling and after 50 cycles. Inset shows the equivalent circuit model for the battery system.

REFERENCES

(1) Sun, H.; Wang, W.; Yu, Z.; Yuan, Y.; Wang, S.; Jiao, S. A New Aluminum-Ion Battery with High Voltage, High Safety and Low Cost. *Chem. Commun.* **2015,** *51*, 11892-11895.

(2) Chen, H.; Guo, F.; Liu, Y.; Huang, T.; Zheng, B.; Ananth, N.; Xu, Z.; Gao, W.; Gao, C. A Defect-Free Principle for Advanced Graphene Cathode of Aluminum-Ion Battery. *Adv. Mater.* **2017,** *29*, 1605958.

(3) Chen, H.; Chen, C.; Liu, Y.; Zhao, X.; Ananth, N.; Zheng, B.; Peng, l.; Huang, T.; Gao, W.; Gao, C. High-Quality Graphene Microflower Design for High-Performance Li-S and Al-Ion Batteries. *Adv. Energy Mater.* **2017,** *7*, 1700051.

(4) Yu, X.; Wang, B.; Gong, D.; Xu, Z.; Lu, B. Graphene Nanoribbons on Highly Porous 3D Graphene for High-Capacity and Ultrastable Al-Ion Batteries. *Adv. Mater.* **2017,** *29*, 1604118.

(5) Jayaprakash, N.; Das, S.; Archer, L. The Rechargeable Aluminum-Ion Battery. *Chem. Commun.* **2011,** *47*, 12610-12612.

(6) Wang, W.; Jiang, B.; Xiong, W.; Sun, H.; Lin, Z.; Hu, L.; Tu, J.; Hou, J.; Zhu, H.; Jiao, S. A New Cathode Material for Super-Valent Battery Based on Aluminum Ion Intercalation and Deintercalation. *Sci. Rep.* **2013,** *3*, 3383.

(7) Koketsu, T.; Ma, J.; Morgan, B. J.; Body, M.; Legein, C.; Dachraoui, W.; Giannini, M.; Demortière, A.; Salanne, M.; Dardoize, F. Reversible Magnesium and Aluminum Ions Insertion in Cation-Deficient Anatase TiO_2. *Nat. Mater.* **2017,** *16*, 1142-1148.

(8) Cohn, G.; Ma, L.; Archer, L. A. A Novel Non-Aqueous Aluminum Sulfur Battery. *J. Power Sources* **2015,** *283*, 416-422.

(9) Yu, Z.; Kang, Z.; Hu, Z.; Lu, J.; Zhou, Z.; Jiao, S. Hexagonal NiS Nanobelts as Advanced Cathode Materials for Rechargeable Al-Ion Batteries. *Chem. Commun.* **2016,** *52*, 10427-10430.

(10) Wang, S.; Jiao, S.; Wang, J.; Chen, H.-S.; Tian, D.; Lei, H.; Fang, D.-N. High-Performance Aluminum-Ion Battery with CuS@C Microsphere Composite Cathode. *ACS Nano* **2017,** *11*, 469-477.

(11) Hu, Y.; Luo, B.; Ye, D.; Zhu, X.; Lyu, M.; Wang, L. An Innovative Freeze-Dried Reduced Graphene Oxide Supported SnS_2 Cathode Active Material for Aluminum-Ion Batteries. *Adv. Mater.* **2017,** *29*, 1606132.

(12) Lei, H.; Jiao, S.; Tu, J.; Song, W.-L.; Zhang, X.; Wang, M.; Li, S.; Chen, H.; Fang, D. Modified Separators for Rechargeable High-Capacity Selenium-Aluminum Batteries. *Chem. Eng. J.* **2020,** *385*, 123452.

(13) Jiang, J.; Li, H.; Fu, T.; Hwang, B.-J.; Li, X.; Zhao, J. One-Dimensional $Cu_{2-x}Se$ Nanorods as the Cathode Material for High-Performance Aluminum-Ion Battery. *ACS Appl. Mater. Interfaces* **2018,** *10*, 17942-17949.

(14) Li, G.; Tu, J.; Wang, M.; Jiao, S. Cu_3P as a Novel Cathode Material for Rechargeable Aluminum-Ion Batteries. *J. Mater. Chem. A* **2019,** *7*, 8368 –8375.

(15) Jiao, H.; Tian, D.; Li, S.; Fu, C.; Jiao, S. A Rechargeable Al-Te Battery. *ACS Appl. Energy Mater.* **2018,** *1*, 4924-4930.